

Supporting Information

Coordination Strategy to Achieve Instant Dissolution of a Biomedical Polymer in Water via Manual Shaking

*Jingyu Tang, Caiyun Cai, Dinglingge Cao, Weihan Rao, Wen Guo, Lin Yu and Jiandong Ding**

State Key Laboratory of Molecular Engineering of Polymers, Department of Macromolecular Science, Fudan University, Shanghai 200438, China.

Email: jdding1@fudan.edu.cn

This PDF file includes:

Supplementary Materials and Methods

Supplementary Results with Figures S1 to S14 and Tables S1 to S2 shown in sequence mentioned in the main manuscript

Supplementary References

S1. Supplementary Materials and Methods

S1.1 Supplementary Materials.

Poly(ethylene glycol) (PEG) with number average molecular weight M_n 1500 (PEG-1500) and stannous 2-ethyl-hexanoate ($\text{Sn}(\text{Oct})_2$, 95%) were purchased from Sigma-Aldrich. D, L-lactide (LA) and glycolide (GA) were provided by Hangzhou Medzone Biotech CO., Ltd. (Zhejiang, China). Anhydrous calcium chloride (CaCl_2 , 96%), trisodium citrate ($\text{C}_6\text{H}_5\text{Na}_3\text{O}_7$, 98%), and tetrahydrofuran ($\text{C}_4\text{H}_8\text{O}$, chromatographic grade) were from Sinopharm Chemical Reagent Co., Ltd. (Shanghai, China). Buffered paraformaldehyde (4%) was from Boster, INC, China. Dulbecco's modified eagle medium (DMEM), fetal bovine serum (FBS), penicillin and streptomycin were purchased from ThermoFisher Scientific. Normal saline and cell counting kit (CCK-8) were from Beyotime Biotechnology.

S1.2 Experimental animals and cell lines.

ICR mice (male, 25 ± 2 g) and healthy experimental rabbits (male, 2 ± 0.2 kg) were provided by Shanghai Institute of Pharmaceutical Industry, China. The animals experienced free access to water and food in experiment animal room with a light control of 12 h darkness and 12 h light cycle.

S1.3. Synthesis of PLGA-*b*-PEG-*b*-PLGA triblock copolymer.

The triblock copolymer was synthesized via bulk ring-opening copolymerization. Briefly, 29.4 g PEG-1500 was dehydrated in a flask by vacuum at 120°C for 2 h. After the flask was cooled to 80°C , 58.8 g of LA, 11.8 g of GA and 0.25 g of $\text{Sn}(\text{Oct})_2$ were added under an argon protection. Then the argon was exchanged with vacuum for three times to eliminate the residual moisture. The reaction system was then stirred continuously at 140°C under an argon atmosphere. After 12 h of reaction, the raw product was washed with three folds amounts of water at 80°C for three times to eliminate residual monomers. The obtained polymer was directly dissolved in water with continuous magnetic stirring at 4°C . Solid PLGA-*b*-PEG-*b*-PLGA triblock copolymer was obtained through freeze-drying.

S1.4. Preparation of calcium coordinated polymers.

Aqueous solutions of PLGA-*b*-PEG-*b*-PLGA with a concentration of 50 mg/mL were added with different amounts of CaCl_2 to obtain mixture solutions. The mixtures were then frozen at -20°C for 12 h followed by freeze-drying for another 48 h. After that, calcium coordinated polymers (Polymer/Ca samples) were obtained. As controls, copolymer composites with NaCl or glucose, and PEG/Ca composite were prepared with a similar method.

S1.5. Dissolution experiments in water and in acetone.

Solid PLGA-*b*-PEG-*b*-PLGA triblock copolymer, calcium coordinated polymers and the control samples were dissolved in water via manual shaking or via continuous magnetic stirring at 4°C. In addition, the triblock copolymer and the calcium coordinated samples were also dissolved in acetone by shaking and a laser was illuminated through the solution to examine Tyndall effect.

The dissolution properties of PEG/Ca and Polymer/Ca (100:50) in acetone were studied to obtain the dissolved fraction of PEG/Ca in acetone, the molar ratios of LA (-C_HCH₃COO-), GA (-CH₂COO-) to the chain unit of PEG block (-CH₂CH₂O-) as well as the final molar ratio of oxygen atoms in polymer (O_{Polymer}), PLGA block (O_{PLGA}), PEG block (O_{PEG}) to total calcium atoms.

S1.6. Characterizations of the polymer systems.

The synthesized PLGA-*b*-PEG-*b*-PLGA was detected in a 400 MHz ¹H NMR spectrometer (Bruker, AVANCE III HD) using CDCl₃ as the solvent and tetramethylsilane as the internal standard. M_n , weight average molecular weight M_w and molar mass dispersity D_M were detected with a GPC (Agilent 1260) system equipped with a detector of differential refractometer. A flow rate of 1 mL/min tetrahydrofuran was used as the eluent and monodispersed polystyrene served as the standard for molecular weight calibration. The D_M value of the PLGA block was calculated according to the tested D_M results of PEG and the corresponding block copolymer using the formula in the literature.^{S1}

The appearances of different samples were captured using a digital camera. The morphology analysis and component detection were taken in an scanning electron microscope (Tescan, VEGA 3 XMU) equipped with an EDS (Bruker, Quantax200 XFIASH6/60). The freeze-dried samples were coated with a thin layer of evaporated gold, and then tested at an accelerating voltage 30 kV.

The further chemical structures were analyzed with an FTIR (Thermofisher, Niclet 6700) of resolution 0.09 cm⁻¹. The samples were tableted with pure KBr powder and then the transmittance at 500~4000 cm⁻¹ were detected.

The X-ray diffraction spectra were recorded in a diffractometer (Bruker, D2 PHASER) with Cu-K α radiation. The test voltage and current were 30 kV and 10 mA, respectively. Diffraction intensity from 2 θ of 10° to 80° was recorded.

DSC analysis was carried out in a DSC analyzer (TA, Q2000) with a thermal sensitivity of 0.2 μ W and a temperature accuracy of $\pm 0.1^\circ\text{C}$. The sample was placed in an alumina oxide

pan and then heated to 160 °C with a ramping rate of 20°C/min under an inert nitrogen protection of 50 mL/min. Then the sample was kept at 160 °C for 0.5 min to eliminate the thermal history followed by cooling to -60 °C with a rate of 20°C/min. After isothermal maintenance at -60 °C for 0.5 min, another heating to 160°C with a ramping rate of 20°C/min was applied. Data of the first cooling cycle and the second heating process were collected.

The chemical environments of the surface elements were tested in an X-ray photoelectron spectroscope (PHI, PHI 5000C) with Mg-K α radiation and a pass energy of 93.9 eV. All XPS data were calibrated to C 1s core peak and then analyzed using PeakFit v4.12 software. The peak fit follows the literature.^{S2}

Aqueous solutions with polymer concentration of 10 mg/mL were used for dynamic laser scattering measurement and ζ -potential analysis in a DLS apparatus (Malvern, Zetasizer Nano ZS90). Prior to measurements, the solutions were filtrated with 0.45 μ m filters to remove possible dusts and then equilibrated at 25°C for at least 20 min. A scattering angle of 90° and an argon ion laser of 532 nm were selected for the following measurements. The average diameter was obtained according to the volume distribution data. Three parallel tests were applied for each group. The acetone solution of Polymer/Ca with a solid content of 5 mg/mL was also tested by DLS.

Critical micelle concentration (CMC) was tested using a hydrophobic dye 1, 6-diphenyl-1, 3, 5-hexatriene (DPH). Briefly, methanol solutions of DPH were added into polymer solutions to form test solutions with final DPH concentration of 4 μ M and final polymer concentrations of 0.00001%-0.5% (w/v). After equilibrated at 4°C for 12 h, the absorption differences at 377 nm and 400 nm of the solutions were tested in a UV-vis spectrophotometer (Malvern, TU1950). CMC was determined as the concentration with a significant increase of the absorption difference.

Transmission electron microscopy (TEM) in a microscope (Hitachi, HT7800) was used to observe the micelles of calcium coordinated polymers formed in water and acetone. Briefly, an aqueous solution of 50 mg/mL PLGA-*b*-PEG-*b*-PLGA loaded with CaCl₂ were dripped onto a copper-grid film and then freeze-dried following the process of preparation of calcium coordinated polymers. In order to perform better TEM observations, the freeze-dried samples loaded on copper-grid films were gently vibrated by knocking with a tweezers to remove the over loaded composites. Then the TEM images were acquired at an accelerating voltage of 200 kV. Similarly, the acetone solution of 5 mg/mL PLGA-*b*-PEG-*b*-PLGA and 5 mg/mL calcium coordinated composites were dripped onto copper-grid films and dried at room temperature for at least 24 h followed by the TEM observations.

The gelation properties of different aqueous solutions were tested with a vial inverting method. Briefly, 0.5 mL aqueous solutions with different sample concentrations in 2 mL vials were immersed in a water bath at each temperature for 10 minutes. Then the vials were inverted and the gel state were determined if no flow occurred in 30 s. The tests were performed from temperature of 25°C to 50°C with an increase of 1°C per step. Finally, phase diagrams were drawn according to the results from the vial inverting method. Three parallel tests were applied for each group.

The rheological properties of aqueous polymer solutions were tested in a strain-controlled rheometer (Malvern, KNX2100) using a Peltier cone-plate (1°, 60 mm in diameter, 0.03 mm in gap). Samples were loaded onto the plate with a thin layer of silicone oil protection to avoid water evaporation. The tests were performed with an oscillatory frequency of 1.59 Hz and a temperature increase rate of 1°C /min from 15°C to 45°C.

We also recorded in vitro release of calcium ions from different gels. Briefly, aqueous solutions with polymer concentration of 15% (w/v) were prepared, and then 1 mL of these solutions were added into 15 mL glass vials. The vials were incubated in a water bath of 37°C with a shaking rate of 50 rpm for 10 min, after which 10 mL PBS (0.01 M, pH 7.4) containing 0.025% NaN₃ was added into each vial as the release medium. The release medium (4 mL) was collected, and the same volume of fresh PBS was supplemented into the vial at each predetermined time point. Three parallel vials were set for each group. The released calcium was tested by an inductively coupled plasma optical emission spectrometer (ICP-OES, Thermofisher Scientific, iCAP 7400). Prior to the test, the sample mediums were treated with 20% nitric acid solution at room temperature for 12 h.

For in vitro cytotoxicity evaluation, aqueous solutions with final polymer concentration of 15% (w/v) of PLGA-*b*-PEG-*b*-PLGA and Polymer/Ca as well as sodium citrate solutions of Polymer/Ca (final polymer concentration of 15% (w/v)) were filtrated through poly(ether sulfone) (PES) membrane filters (Millipore Express, 0.22 µm) to remove bacteria. NIH 3T3 cells (1×10⁴ per well) were seeded into 96-plates and then cultured with 100 µL culture medium of DMEM containing 10% (v/v) FBS, 100 U/mL penicillin and 100 µg/mL streptomycin in each well. After 24 h of incubation in a 5% CO₂, humid atmosphere at 37°C, the culture media were completely replaced with fresh culture media containing different amounts of samples; the final polymer concentrations were 1-10 mg/mL, which were obtained via addition of different solutions into culture media. For each group, *n* = 6. After another 24 h of incubation, the culture media were collected for assays of pH and molar osmotic pressure. The cells in plates were further incubated with DMEM containing 10% (v/v) CCK-8 for 2 h. The absorbance

values at 450 nm of each well were then measured in a microplate reader (Biotek, ELx808). Cells in culture media without any sample served as the negative control and the cell viability was recognized as 100%. The pH values of cell culture media containing samples as well as the collections after cell culture were tested with a pH detector (Mettler Toledo, FiveEasy Plus) and the molar osmotic pressures were measured with an auto F. P. Osmometer (Shanghai Medical University Instrument Co., Ltd., FM-8P). The cytotoxicity evaluation was also carried out using the cell culture medium extracts from different gels. Briefly, 1 mL sample solution with polymer concentration of 15% (w/v) in a 15 mL vial was kept in a water bath of 37°C with a shaking rate of 50 rpm for 10 min to form a gel. Then 5 mL cell culture medium was added followed by further 24 h of incubation. The obtained cell culture medium extracts were then used for cell viability measurements.

For in vitro hemocompatibility evaluation, a whole blood from a male healthy experimental rabbit was used to evaluate the hemolysis of different gels and solutions. The whole blood was collected from a male healthy experimental rabbit using a 5 mL blood-collection tube containing 3.8% (w/v) sodium citrate. We then distilled 4 mL of the whole blood by 10 mL normal saline for further use. The sample solution of 1 mL was gelled at the bottom of a 15 mL tube for 10 min of incubation at 37°C followed by addition of 10 mL normal saline. We set 10 mL normal saline and 10 mL distilled water in empty tubes as negative and positive controls, respectively. After 30 minutes of further incubation at 37°C, 0.2 mL diluted blood mentioned above was added and further cultured at 37°C for 60 min. The liquid was then collected into a centrifuge tube and centrifuged at 800 g for 5 min. The absorbance at 545 nm of the obtained supernatant was measured in a UV-vis spectrophotometer (Malvern, TU1950). The hemolytic fraction was then calculated by using the following formula:

$$\text{Hemolysis (\%)} = \frac{OD_{\text{sample}} - OD_{\text{negative}}}{OD_{\text{positive}} - OD_{\text{negative}}} \times 100 \quad (\text{S1})$$

Here, OD_{negative} , OD_{positive} and OD_{sample} are the optical densities of the negative control, the positive control and the tested sample, respectively.

In addition, the hemolysis evaluations were also carried out after direct incubation of blood with polymer solutions. Briefly, a sample solution of polymer concentration 15% (w/v) was added into 10 mL normal saline to form a mixture with the final polymer concentration of 1 mg/mL. After co-cultured with 0.2 mL diluted blood at 37°C for 60 min, the hemolysis fraction was determined by similar procedure as mentioned above. All hemolysis tests were analyzed in triplicate.

For in vivo biocompatibility assay, sample solutions were subcutaneously injected into both sides of the backs of male ICR mice to form in situ gels. The total injected volume of each mouse was 0.2 mL (0.1 mL/position). At each predetermined time point, the skin tissues containing gels of two mice (four skin tissues in total) were harvested for further histological analysis. Briefly, the harvested tissues were first fixed in 4% buffered paraformaldehyde for 24 h, and then embedded in paraffin followed by section using a rotary microtome (Leica, RM2235). The sections were stained with H&E following the standard procedures in the instruction. The final images were observed in an optical microscope (ZEISS, Axiovert 200)

S1.7 Density functional theory calculations.

The geometry optimizations of all coordination complexes were calculated using the mixing basis set consisting of Def2TZVP for Ca atom and Def2SVP for other atoms. The binding strength was obtained by calculating the corresponding Gibbs-free energy differences before and after calcium coordination with chain segments of PEG, PLA and PGA, using Def2TZVP basis set for all atoms in the theoretical level of the M06-2X hybrid functional with the D3 long-ranger-dispersion correction, in Gaussian 09 software package for density functional theory (DFT).^{S3-S4}

S1.8. Computational characterization of the interaction of calcium ions with two polymer blocks, PLGA and PEG.

In order to reveal the self-assembly properties of PLGA-*b*-PEG-*b*-PLGA (PEG: poly(ethylene glycol); PLGA: poly(lactide-*co*-glycolide)) and the calcium agent in water and acetone, we also examine the dissolution properties of the homopolymer PEG and CaCl₂. To this end, we prepared the composite PEG/Ca, and added 0.4 g PEG/Ca into 8 mL acetone. After 12 h of static treatment, the insoluble product was collected for weighing. The dissolved fraction of PEG/Ca in acetone was calculated according to the following formula:

$$\text{Dissolved fraction} = \frac{0.4 - M_p}{0.4} \times 100\% \quad (\text{S2})$$

Here, M_p indicates the mass of the insoluble product in units of gram.

Polymer/Ca (100:50), namely, the composite of polymer and calcium chemical (here CaCl₂) with weight ratio 100:50, was also dissolved into acetone via manual shaking, forming a mixture with a solid content of 10 mg/mL. Then, after 12 h of static treatment, the precipitate and the solution were separated. The acetone was removed via volatilization at 50°C. The content of calcium (wt%) in the net separation was tested using a calcium colorimetric assay kit (Beyotime). Briefly, 10 folds amount of ethanol was added into the separation to extract calcium out; then the calcium in the extraction was tested.

The polymer obtained after ethanol treatment was analyzed based on hydrogen spectrum of nuclear magnetic resonance ($^1\text{H-NMR}$, Bruker, AVANCE III HD) to obtain the molar ratio of LA ($-\text{CHCH}_3\text{COO}-$), GA ($-\text{CH}_2\text{COO}-$) to the chain unit of PEG block ($-\text{CH}_2\text{CH}_2\text{O}-$). The final molar ratio of oxygen atoms in polymer (O_{Polymer}), PLGA block (O_{PLGA}), PEG block (O_{PEG}) to total calcium atoms were calculated by the following formulas:

$$O_{\text{Polymer}}/\text{Ca} = \frac{(1 - wt) \times 111 \times (1 + 2 \times nLA + 2 \times nGA)}{(44 + 72 \times nLA + 58 \times nGA) \times wt} \quad (\text{S3})$$

$$O_{\text{PEG}}/\text{Ca} = \frac{(1 - wt) \times 111}{(44 + 72 \times nLA + 58 \times nGA) \times wt} \quad (\text{S4})$$

$$O_{\text{PLGA}}/\text{Ca} = \frac{(44 + 72 \times nLA + 58 \times nGA) \times wt}{(1 - wt) \times 111 \times (2 \times nLA + 2 \times nGA)} \quad (\text{S5})$$

Here, “wt” was the content of calcium (wt%) in the net separation, which was tested with a calcium colorimetric assay kit (Beyotime); nLA and nGA were the molar ratios of LA ($-\text{CHCH}_3\text{COO}-$), GA ($-\text{CH}_2\text{COO}-$) to the chain unit of PEG ($-\text{CH}_2\text{CH}_2\text{O}-$) obtained from ^1H NMR.

S1.9 Ex vivo test of ESD in a porcine stomach.

Polymer/Ca (100:15) was rapidly dissolved in an aqueous medium containing sodium citrate and indigo carmine (0.5 wt%) by manual shaking to form a solution with final polymer concentration of 15% (w/v) and final molar ratio of calcium to citrate of 4:1. A porcine stomach was cut into 5×5 cm squares and then flatly fixed on a plastic board. We used a 20 mL syringe with a 23-gauge needle to submucosally inject 5 mL solution to elevate the mucosa. The injection pressure was read with a pressure gauge (True Tech Medical Co. Ltd., Guangdong, China). The height of the elevation was recorded with a Vernier caliper at the preset time points. The porcine stomach squares were kept in a bath of normal saline at 37°C during the whole procedure. Three parallel tests were carried out for each sample.

S1.10. Statistical analysis.

One-way t -test was used for comparison of the collected data. The calculated $p < 0.05$ presents a significant difference between the examined two groups.

S2. Supplementary Results

S2.1 Characterization of the synthesized copolymer. The chemical structure and the $^1\text{H-NMR}$ spectrum of the synthesized PLGA-*b*-PEG-*b*-PLGA triblock copolymer are shown in **Figure S1**. The integral areas of the characteristic peaks at chemical shifts of 5.20 ppm ($-\text{CH}(\text{CH}_3)\text{COO}-$, peak a), 4.80 ppm ($-\text{CH}_2\text{COO}-$, peak c), 3.60 ppm ($-\text{CH}_2\text{CH}_2\text{O}-$, peak d) and 1.55 ppm ($-\text{COCH}(\text{CH}_3)\text{O}-$, peak b) were used to calculate the molecular parameters.

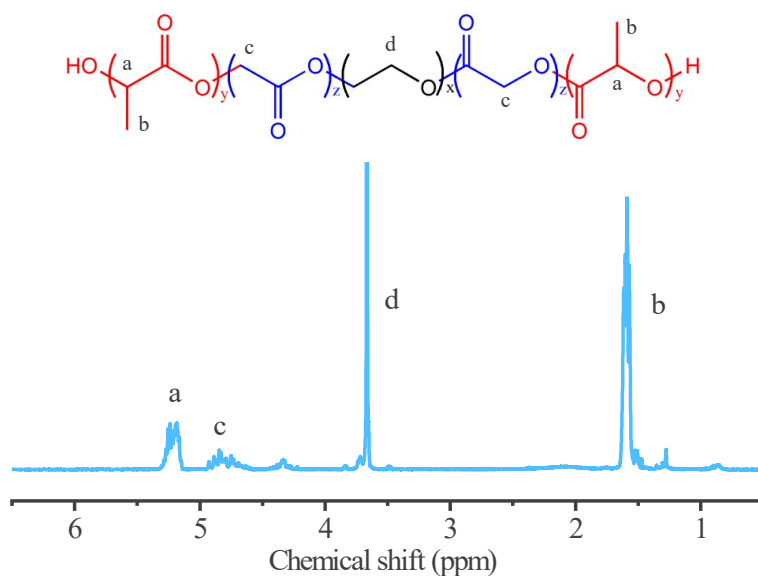
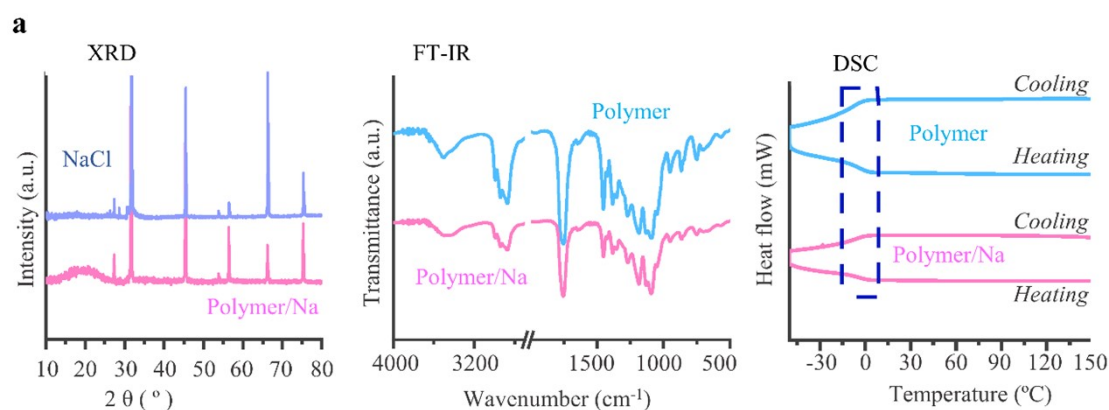


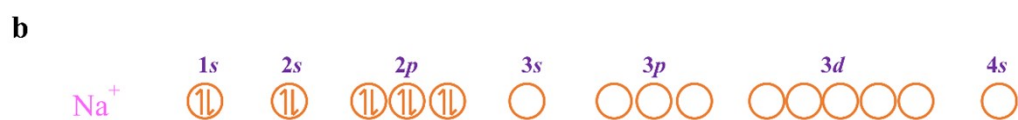
Figure S1. ¹H-NMR spectrum of the synthesized polymer.

S2.2 Physicochemical properties. We carried out a series of characterizations such as XRD. As shown in **Figure S2a**, NaCl showed crystal diffraction peaks at 2θ of 31.8° , 45.5° , 53.8° , 56.5° and 66.3° . For Polymer/Na (100:20), the increased background intensities of polymer and all the diffraction peaks of NaCl crystal were clearly observed. The results indicates that Polymer/Na was a mixture of polymer and NaCl crystal.

Figure S2 also shows the FT-IR spectra; the detailed wavenumbers and their assignments are listed in **Table S1**. Polymer and Polymer/Na (100:20) exhibited similar FT-IR spectra. The characteristic peaks at 1051 cm^{-1} , 1092 cm^{-1} and 1185 cm^{-1} correspond to the C-O stretching; the characteristic peaks at 1755 cm^{-1} and 2875 cm^{-1} refer to the C=O stretching and the CH_2 stretching, respectively.



No significant difference between Polymer and Polymer/Na was observed from the XRD, FT-IR and DSC results.



Na^+ can not attract the lone pair electrons of the oxygen atoms of PLGA-*b*-PEG-*b*-PLGA into its empty orbits.

Figure S2. Analysis of Polymer/Na. **(a)** XRD, FT-IR and DSC results of Polymer and Polymer/Na. The corresponding spectra of XRD, FT-IR and DSC have been properly vertically moved for clear display. **(b)** The electronic structure of Na^+ .

Table S1 The detailed wavenumbers of the characteristic absorption peaks in FT-IR and their assignments for Polymer, Polymer/Ca and Polymer/Na.

Polymer (cm^{-1})	Polymer/Na (cm^{-1})	Polymer/Ca (cm^{-1})	Assignment
1051	1052	1052	C-O stretch
1092	1093	1089	C-O stretch
1130	1130	1132	C-C stretch
1185	1185	1190	C-O stretch
1270	1270	1272	CH_2 wag
1383	1382	1385	CH_3 scissor
1453	1453	1453	CH_2 , CH_3 scissor
1755	1755	1760	C=O stretch
2875	2876	2889	CH_2 stretch
2994	2993	2996	CH_3 stretch

Polymer and Polymer/Na also showed similar DSC curves (Figure S2a). No melting and crystallization peaks were observed among the examined temperatures.

The electronic structure of sodium ion is schematically presented in Figure S2B. As compared with calcium ion, the lower atomic number and charges could not lead to coordination with the oxygen atoms of PLGA-*b*-PEG-*b*-PLGA.

The surface atom chemical environments in Polymer and Polymer/Ca were tested by XPS. In the C 1s XPS traces (**Figure S3**), the Polymer exhibited four spectral components at binding energies of 285.05 eV, 286.39 eV, 287.36 eV and 289.29 eV corresponding to -CH₃, -CH₂-O-, -CH-O-, and -C=O groups, respectively. Polymer/Ca also exhibited these four spectral components; the C 1s binding energy of -CH₂-O- group read 286.05 eV, which was 0.34 eV smaller than that of Polymer. The C 1s binding energies of the other three groups were similar to those of Polymer.

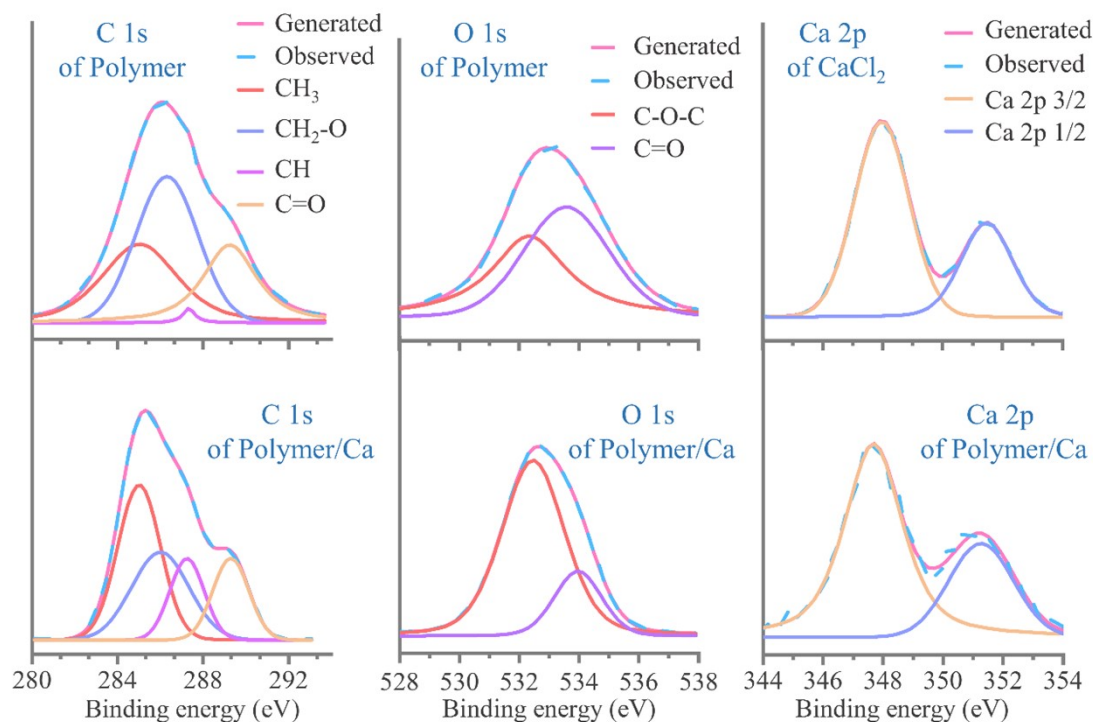


Figure S3. High resolution XPS traces of C 1s and O 1s of Polymer and Polymer/Ca as well as Ca 2p of Polymer/Ca and CaCl₂. The O 1s binding energies of O=C and C-O-C in Polymer/Ca turned 0.2 eV and 0.4 eV bigger than the corresponding results of Polymer. The Ca 2p binding energy of Polymer/Ca was smaller than the corresponding result of CaCl₂.

In the O 1s XPS traces, both Polymer and Polymer/Ca possessed two spectral components. The binding energies of -C=O and C-O-C groups in Polymer/Ca were 532.49 eV and 533.99 eV, respectively, which were 0.19 eV and 0.43 eV higher than those of Polymer (532.30 eV and 533.56 eV). In the Ca 2p XPS traces, the binding energy of Polymer/Ca was 0.31 eV smaller than the result of CaCl₂ (343.67 eV and 347.98 eV, respectively). The binding energy data revealed by XPS are summarized in **Table S2**.

Table S2 Binding energies of C 1s, O 1s in Polymer (EB_P), Polymer/Ca ($EB_{P/Ca}$) as well as their differences ($EB_{P/Ca} - EB_P$) revealed by XPS measurements.

Peaks	EB_P (eV)	$EB_{P/Ca}$ (eV)	$EB_{P/Ca} - EB_P$ (eV)
C 1s (CH_3)	285.05	285.09	+0.04
C 1s (CH_2-O)	286.39	286.05	-0.34
C 1s ($CH-O$)	287.36	287.30	-0.06
C 1s ($C=O$)	289.29	289.30	-0.01
O 1s ($C=O$)	532.30	532.49	+0.19
O 1s ($C-O-C$)	533.56	533.99	+0.43
Ca 2p 1/2	351.52^a	351.28	-0.24^b
Ca 2p 3/2	347.98^a	347.67	-0.31^b

^a Binding energy of Ca 2p in $CaCl_2$ (noted as EB_{Ca}). ^b $EB_{P/Ca} - EB_{Ca}$

S2.3. Dissolution in acetone for the mechanism study. To analyze the molecular interactions in the coordinated samples, a dissolution test in acetone was carried out. Some results are presented in **Figure S4**. Polymer could be easily dissolved in acetone forming a molecular solution; NaCl was insoluble in acetone; Polymer/Na could only be partially dissolved in acetone resulting in a molecular solution of polymer and a precipitate of NaCl.



Figure S4. Dissolution of Polymer, NaCl and Polymer/Na in acetone.

The diluted acetone solutions were further analyzed by TEM. As shown in **Figure S5**, no micelle was observed for acetone solutions of Polymer; in contrast, for acetone solutions of Polymer/Ca (100:15), micelles were clearly observed. The Polymer/Ca (100:15) solid obtained by freeze-drying of the mixed aqueous solution of polymer and $CaCl_2$ (polymer concentration of 50 mg/mL) also showed a large number of micelles, which illustrated the existence of micelles in Polymer/Ca composite.

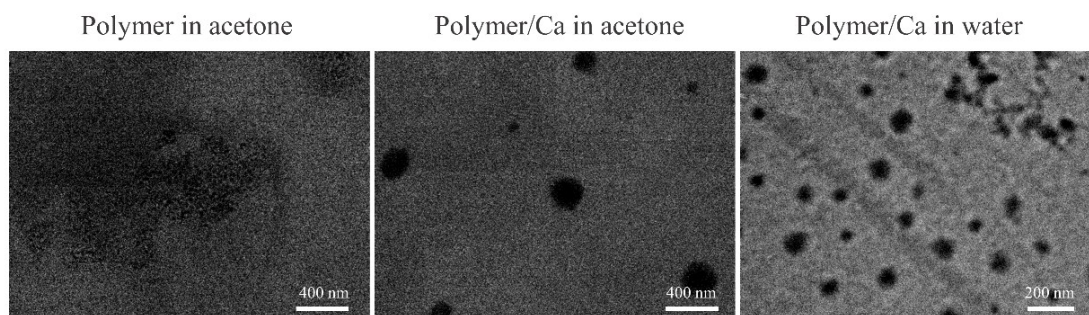


Figure S5. TEM images corresponding to the acetone solution of Polymer (5 mg/mL), the acetone solution of Polymer/Ca (5 mg/mL) and the aqueous solution of Polymer/Ca (50 mg/mL). Micelles were observed for the acetone solution of Polymer/Ca and the aqueous solution of Polymer/Ca. The observations were made after drying.

We also examined PEG/Ca samples in acetone. As shown in **Figure S6**, the homopolymer PEG could be completely dissolved in acetone, and PEG/Ca could only be partially dissolved. The dissolution ratio of PEG/Ca decreased with the increase of molar ratio of Ca/O. The values were significantly smaller than the theoretical contents of PEG in PEG/Ca. For example, the PEG content of PEG/Ca with a molar ratio of Ca/O of 20:100 was 67%, but the dissolution ratio of PEG/Ca in acetone was only 36%.

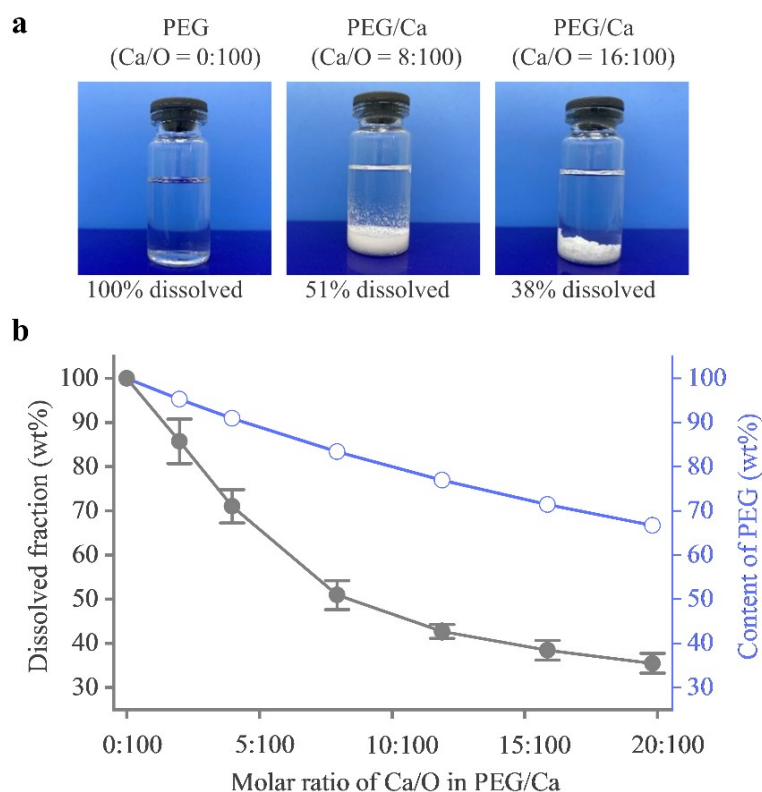


Figure S6. Exploration of calcium coordination with PEG. **(a)** Images of dissolution state of PEG/Ca with different molar ratios of Ca/O in acetone (0.4 g solid sample and 8 mL acetone in

each vial). **(b)** Dissolved fractions of PEG/Ca with different molar ratios of Ca/O in acetone. The dissolvable fraction of PEG/Ca in acetone was much smaller than the PEG content of PEG/Ca, indicating the decrease of solubility in acetone caused by calcium coordination. For each group, $n = 3$.

Further studies illustrated that the composite of the block copolymer PLGA-*b*-PEG-*b*-PLGA and calcium, namely Polymer/Ca (100:50), was partially dissolved in acetone, forming a supernatant of the micelle solution and a precipitate. The supernatant and the precipitate were then dried separately, resulting in two paste-like samples. The $^1\text{H-NMR}$ spectra of the polymer in these two paste-like samples are shown in **Figure S7**. The integral areas of the characteristic peaks at chemical shifts of 5.20 ppm ($-\text{CH}(\text{CH}_3)\text{COO}-$), 4.80 ppm ($-\text{CH}_2\text{COO}-$), 3.60 ppm ($-\text{CH}_2\text{CH}_2\text{O}-$) were used to calculate the molar ratios of LA ($-\text{CHCH}_3\text{COO}-$), GA ($-\text{CH}_2\text{COO}-$) to the chain unit of PEG block ($-\text{CH}_2\text{CH}_2\text{O}-$). The relative integral areas were noted in the $^1\text{H-NMR}$ spectra.

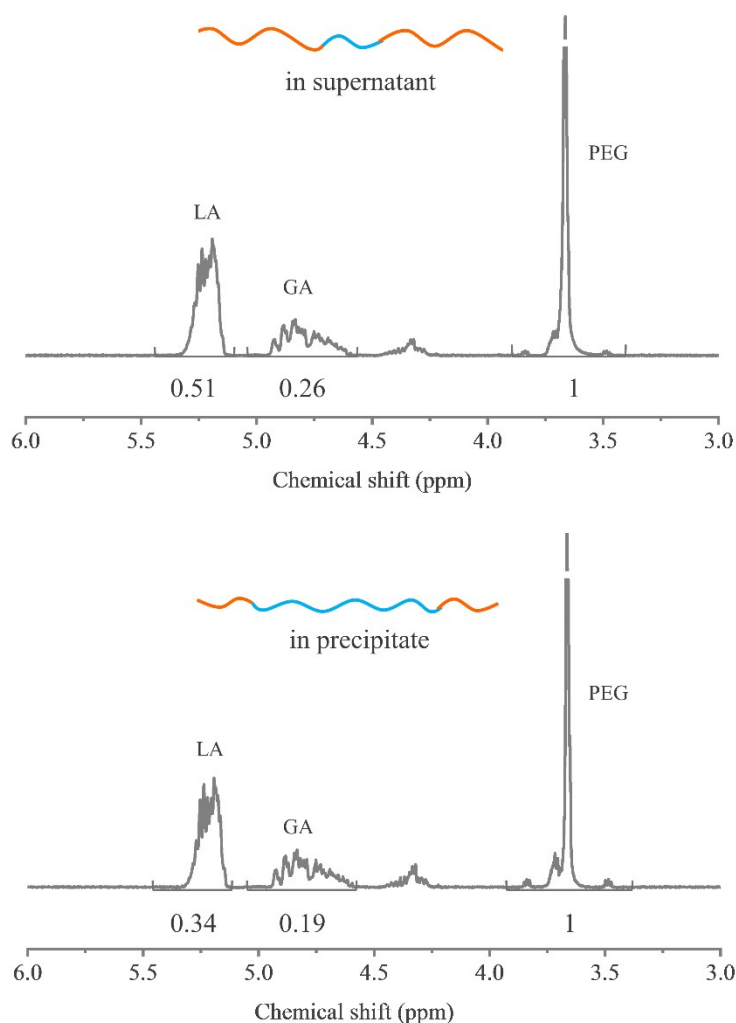


Figure S7. ^1H NMR spectra of the polymers collected from the supernatant of the micelle solution and the precipitate.

S2.4. Chelation strategy to enhance biocompatibility. In cytotoxicity measurements, the pH values of the cell culture media containing different types of samples before and after 24 h of cell culture are shown in **Figure S8a** and the cell viabilities depending on the initial pH values are presented in Fig. S8b. All culture media exhibited the decrease of pH after cell culture. At polymer concentration of 1 mg/mL, the initial pH values before cell culture were similar (8.4-8.6). After culture of cells, the culture medium corresponding to Ternary showed a pH of 7.9, a little lower than the results corresponding to Unitary and Binary (both 8.3). At polymer concentration of 10 mg/mL, the initial pH values were also similar (8.2-8.3). However after 24 h of cell culture, the medium corresponding to Ternary showed the lowest pH of 7.9. The pH value corresponding to Binary was about 8.0, which was lower than the result corresponding to Unitary (8.3). As shown in Figure S8b, for the same types of samples, cell viabilities increased with the increase of initial pH; nevertheless, if compared among different types of samples, no clear correlation between cell viability and initial pH value was found.

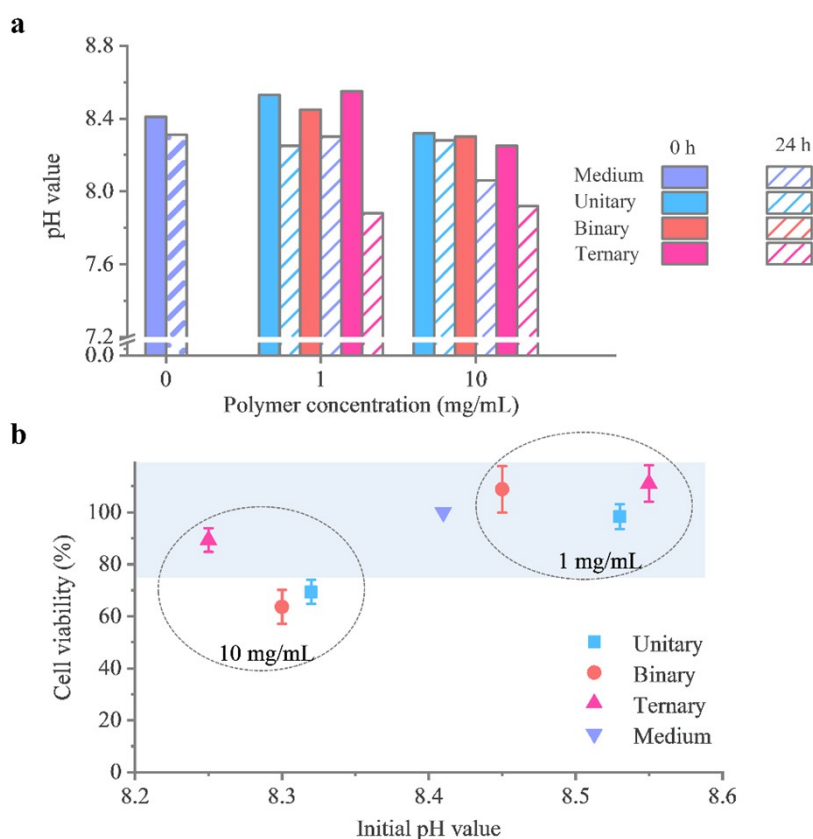


Figure S8. Examination of pH dependence of cell viability. **(a)** pH values of culture media containing different amounts of specimens before and after 24 h of cell cultivation. The pure culture medium served as control. **(b)** Cell viabilities as a function of initial pH for Unitary, Binary and Ternary systems. The results indicate that the better cell viabilities of Ternary was not necessarily pH dependent. For each group, $n = 6$.

We also measured osmolality of cell culture media corresponding to different samples. According to **Figure S9**, all culture media showed osmolality increase after cell culture. At polymer concentration of 1 mg/mL, the initial osmolality results were similar (340-350 mOsmol/kg). After cell culture, medium corresponding to Binary possessed the biggest osmolality about 397 mOsmol/kg and the media corresponding to Ternary and Unitary showed similar osmolality (374 and 377 mOsmol/kg, respectively). At polymer concentration of 10 mg/mL, culture media corresponding to Binary and Ternary showed similar initial osmolalities (348, and 347 mOsmol/kg, respectively) as well as similar final osmolalities after 24 h of cell culture (385, and 384 mOsmol/kg, respectively), which were higher than the results corresponding to Unitary (325 mOsmol/kg before cell culture and 355 mOsmol/kg after cell culture). No obvious correlation between cell viability and initial osmolality was found.

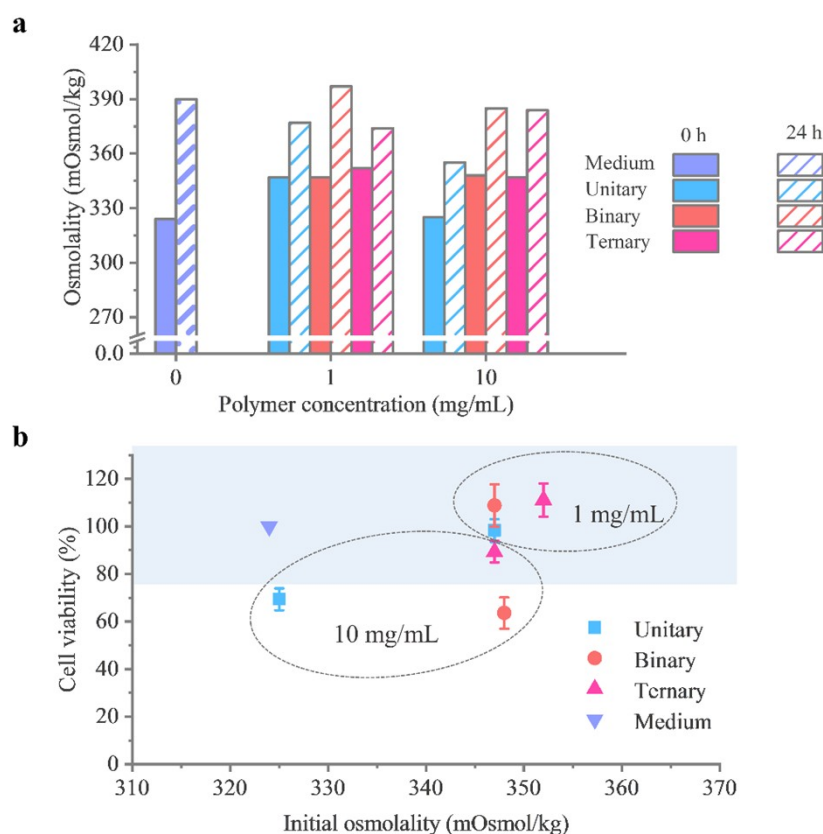


Figure S9. Examination of osmolality dependence of cell viability. **(a)** Osmolality values of the culture media containing different amounts of samples before and after 24 h of cultivation. Pure culture medium was served as control. **(b)** Cell viabilities as a function of initial osmolality values for Unitary, Binary and Ternary systems. The results indicate that the cell viability of Ternary is independent with osmolality. For each group, $n = 6$.

We further performed cytotoxicity measurements of the extracts of three gels, and no significant cytotoxicity was found (**Figure S10**).

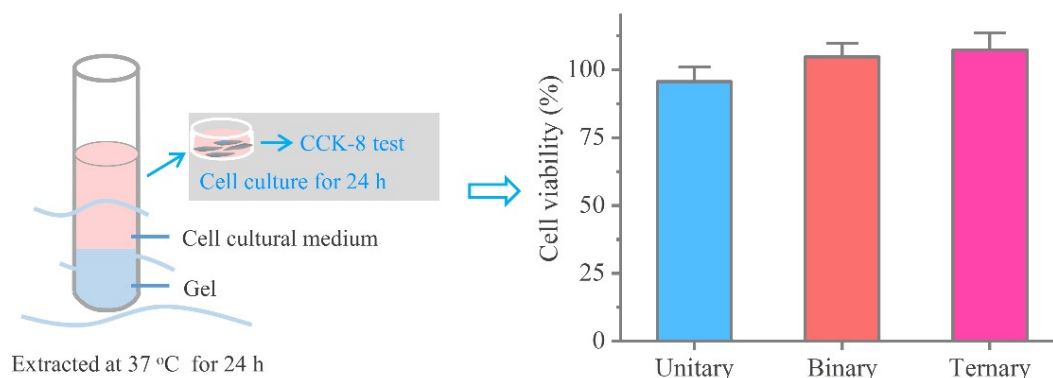


Figure S10. Cytotoxicity results of thermogel extracts. For each group, $n = 6$.

The calcium releases of different gels were detected, and the results are shown in **Figure S11**. The hydrogel of Unitary showed no calcium release reasonably. The gel of Binary showed rapid calcium release to a cumulative calcium release of 21% in the first four days. The release then slowed down during the following 10 days and reached a final cumulative release of 26% at 14 d. For the gel of Ternary, the calcium release was much slower during the examined 14 days, and the final cumulative calcium release was 15%, which were 11% smaller as compared to the results of Binary.

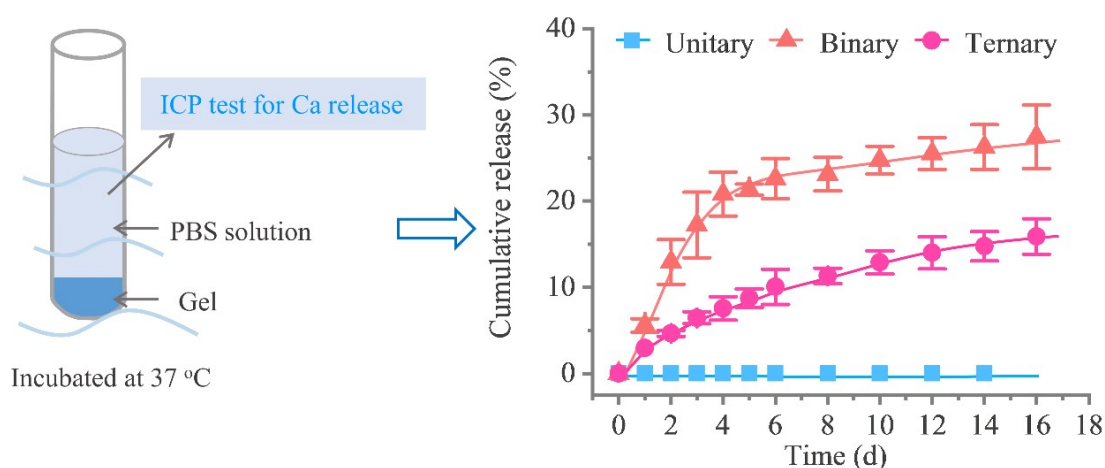


Figure S11. *In vitro* calcium release profiles of Unitary, Binary and Ternary gel systems. For each group, $n = 3$.

We performed H&E imaging to examine *in vivo* inflammatory responses after subcutaneously implanting the hydrogels into mice. According to **Figure S12**, Ternary resulted in the mildest inflammatory response.

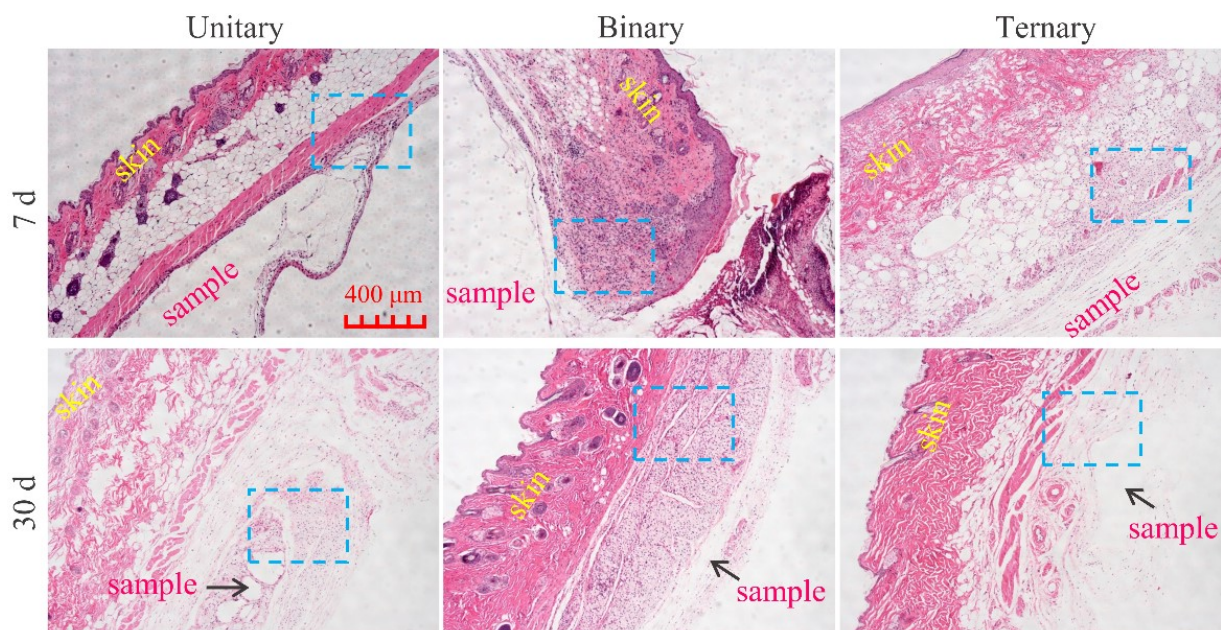


Figure S12. H&E histopathological images after 7 d and 30 d of subcutaneous implantation of Unitary, Binary and Ternary gels. The magnified views of the tissues in the blue dotted rectangles are shown in Fig. 5 in the main manuscript.

The hemolysis values tested by coculture of blood and different samples (final polymer concentration of 1 mg/mL) were all smaller than 5% (**Figure S13**). In addition, the values of hydrogels corresponding to concentrated Unitary, Binary and Ternary were also smaller than 5% (**Figure S14**).

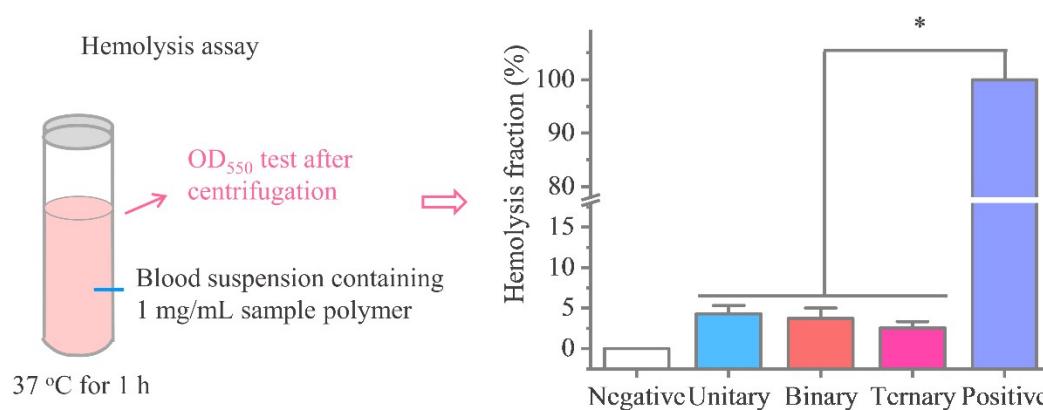


Figure S13. Hemolysis tests by direct incubation of blood suspension with the Unitary, Binary and Ternary systems. The final polymer concentration in blood suspension were all 1 mg/ml. The copolymer concentration of 1 mg/ml is below CGC (not gelled) and well mixed with blood. “*” refers to a significant difference with $p < 0.05$ ($n = 3$).

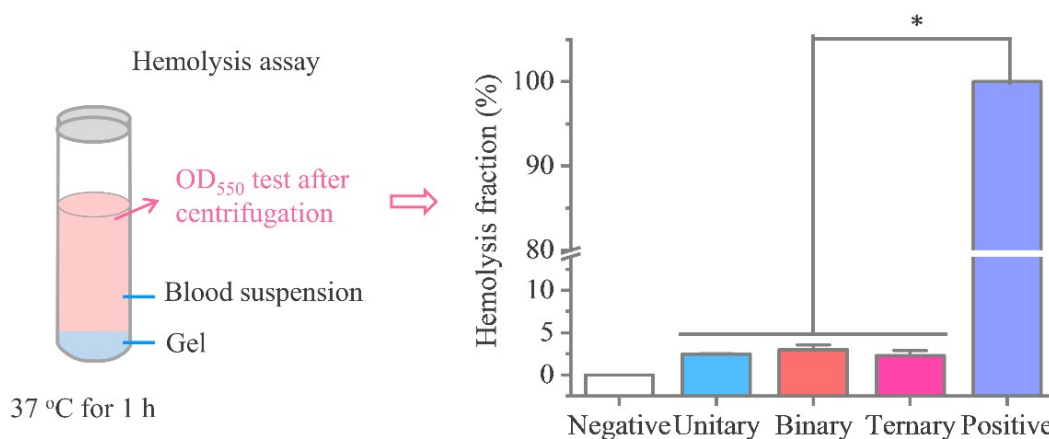


Figure S14. Hemolysis tests of Unitary, Binary and Ternary gels. “*” refers to a significant difference with $p < 0.05$ ($n = 3$).

Supplementary References

- S1. D. Y. Yan, C. Yuan. *Sci. Bull.* **1985**, 24, 1684-1688.
- S2. A. G. Shard, M. C. Davies, Y. X. Li, C. Volland, T. Kissel. *Macromolecules.* **1997**, 30, 3051-3057.
- S3. S. Grimme, J. Antony, S. Ehrlich, H. Krieg. *J. Chem. Phys.* **2010**, 132, 154104.
- S4. Gaussian 09, Revision D.01, Frisch, M. J.; Trucks, G. W.; Schlegel, H. B.; Scuseria, G. E.; Robb, M. A.; Cheeseman, J. R.; Scalmani, G.; Barone, V.; Mennucci, B.; Petersson, G. A.; Nakatsuji, H.; Li, X.; Caricato, M.; Marenich, A.; Bloino, J.; Janesko, B. G.; Gomperts, R.; Mennucci, B.; Hratchian, H. P.; Ortiz, J. V.; Izmaylov, A. F.; Sonnenberg, J. L.; Williams-Young, D.; Ding, F.; Lipparini, F.; Egidi, F.; Goings, J.; Peng, B.; Petrone, A.; Henderson, T.; Ranasinghe, D.; Zakrzewski, V. G.; Gao, J.; Rega, N.; Zheng, G.; Liang, W.; Hada, M.; Ehara, M.; Toyota, K.; Fukuda, R.; Hasegawa, J.; Ishida, M.; Nakajima, T.; Honda, Y.; Kitao, O.; Nakai, H.; Vreven, T.; Throssell, K.; Montgomery, J. A.; Jr., Peralta, J. E.; Ogliaro, F.; Bearpark, M.; Heyd, J. J.; Brothers, E.; Kudin, N.; Staroverov, V. N.; Keith, T.; Kobayashi, R.; Normand, J.; Raghavachari, K.; Rendell, A.; Burant, J. C.; Iyengar, S. S.; Tomasi, J.; Cossi, M.; Millam, J. M.; Klene, M.; Adamo, C.; Cammi, R.; Ochterski, J. W.; Martin, R. L.; Morokuma, K.; Farkas, O.; Foresman, J. B. & Fox D. J. Gaussian, Inc., Wallingford CT, **2016**